Melting of a confined monolayer of magnetized beads

J. Schockmel, E. Mersch, N. Vandewalle, and G. Lumay
GRASP, Physics Department, University of Liège, B-4000 Liège, Belgium
(Received 22 January 2013; revised manuscript received 15 May 2013; published 10 June 2013)

We present an experimental model system to study two-dimensional phase transitions. This system is composed of a monolayer of millimetric beads interacting through shor range magnetic dipole-dipole interactions. As the system is athermal, a mechanical agitation is used to produce an erratic motion of the beads. The two-dimensional melting scenario predicted by the Kosterlitz-Thouless-Halperin-Nelson-Young theory is observed. Each phase (liquid-hexatic-solid) has been highlighted with the use of both static and dynamic order parameters. Translational and orientational order are, respectively, estimated through the pair correlation function $g(r)$ and both orientational correlation function $g_6(r)$ and its temporal counterpart $g_6(t)$. We observe two transitions by tuning the applied magnetic field H. First, a loss of translational order without loss of orientational order is observed. This is the signature of the transition from the solid phase to the so-called "hexatic" phase. Finally, the orientational order disappears, leading to a liquidlike structure.

DOI: 10.1103/PhysRevE.87.062201 PACS number(s): 64.70.dj, 05.70.Fh, 45.70.Cc

I. INTRODUCTION

In three dimensions, crystals are characterized by both long range translational and orientational order. The melting in three dimensions (3D) occurs by simultaneous loss of both translational and orientational order in a single phase transition. The situation is different for 2D systems. Indeed, Mermin and Wagner [1] pointed out that, in 2D systems with short range interactions, spontaneous breaking of continuous symmetries is forbidden at finite temperature. This can also be viewed as an instability of the system against thermal fluctuations. A direct consequence of this statement is the lack of long range translational order. On the contrary, Mermin [2] proved that long range orientational order is preserved. These properties lead to a different melting scenario in 2D than in 3D.

Many theoretical models have been developed to understand the melting process in 2D. The most popular one is the Kosterlitz-Thouless-Halperin-Nelson-Young (KTHNY) theory [3–7], which predicts a melting from solid to liquid in two stages. During the first transition, translational order is completely lost but orientational order becomes a quasi-long range order. During the second transition, the orientational order is also completely lost. The intermediate phase is called "hexatic" for a hexagonal lattice. To sum up the different phases and their order according to the KTHNY theory, see Table I. This theory has been a continuous matter of debate during the last 40 years. Many numerical and experimental studies have been carried out [8–20]. Most of them agree with the KTHNY theory without excluding other theories. For a complete review, see Ref. [21].

Previous experiments concerning 2D melting have been performed with thermal model systems such as colloids without interactions [8,9] and with magnetic dipole-dipole interactions [10,11]. The transition from liquid to solid is observed in two stages with the loss of translational and orientational order for each stage, as predicted by the KTHNY theory. These results have been confirmed by numerical simulations [12,13]. Otherwise, experiments have been performed with athermal systems without interaction [14,16,17] (confirmed numerically [15]) and with Coulomb interactions [18,19]. To our knowledge, no athermal system with short range interaction has been experimentally explored. Other experiments have also been performed with a system of ferrofluid spikes [20]. They all noticed that 2D crystals melt according to the KTHNY theory.

In this paper, we propose a model system to study 2D phase transitions in a granular media with short range interactions. Our system consists in a confined 2D assembly of soft ferromagnetic millimetric beads immersed in a tunable external homogeneous magnetic field. Thus, the interaction between two beads is a tunable dipole-dipole interaction which tends to create order. Furthermore, the system is athermal and an agitation is induced by a well controlled mechanical vibration which tends to create disorder. Such a system presents several advantages. First, the mesoscopic scale of the system allows the recording of trajectories of each bead with a classical optical method. Moreover, at this scale a long equilibration time is not required as in colloidal systems. In this paper, we confront this model system to the well-known KTHNY theory.

II. EXPERIMENTAL SETUP

A sketch of the experimental setup is presented in Fig. 1. A set of N spherical metallic beads of diameter $d = 1$ mm is placed on an horizontal frosted glass plate and confined in a 3-cm-diameter hexagonal metallic cell. The plate is shaken horizontally by two loudspeakers oriented in two orthogonal directions. Two 35-Hz sinusoidal noisy signals are produced by these loudspeakers. As shown later, this configuration leads to an erratic motion of each bead in the plane.

The system is placed in the center of two 13-cm-diameter coils in Helmholz configuration. The magnetic field is oriented vertically and is homogeneous. Indeed, the fluctuations of the magnetic field strength are less than 4% in the region of interest. The beads are made of chrome steel (AISI 52100). The applied magnetic field H induces proportional magnetic dipoles moments $m = V\chi_m H$, where V is the volume of the beads and χ_m is the magnetic susceptibility of the particle. The magnetic susceptibility was measured in [22]. They obtained $\chi_m = 3.6$. We consider that each bead has the same magnetic

 ©2013 American Physical Society

TABLE I. Summary of translational and orientational order, given with respective correlation function, for the different phases according to the KTHNY theory. The last row presents 2D patterns illustrating these phases.

Solid	Hexatic	Liquid
Quasi-long range translational order $g_G(r) \sim r^{-\eta_G(T^\star)}$	Short range translational order $g_G(r) \sim \exp(-r)$	Short range translational order $g_G(r) \sim \exp(-r)$
Long range orientational order $g_6(r) = c$	Quasi-long range orientational order $g_6(r) \sim r^{-\eta_6(T^\star)}$	Short range orientational order $g_6(r) \sim \exp(-r)$
	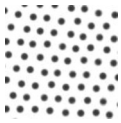	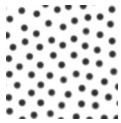

dipolar moment which leads to a repulsive pair potential. One has

$$U_{ij} = \frac{\mu_0}{4\pi}\frac{V^2\chi_m^2 H^2}{r_{ij}^3}, \tag{1}$$

where r_{ij} is the distance between the beads i and j. The repulsive interactions are well controlled by adjusting the strength of the external magnetic field H (from 0 to 14 000 A/m). As the beads are confined in a cell with magnetic walls, when the magnetic field is switched on, the magnetized beads are repelled by the magnetized walls.

In order to obtain a reproducible initial ordered state, the beads are placed in a perfect hexagonal configuration, as shown in the Fig. 4(a), with first neighbor distance $a = 2d$. To form a finite hexagonal lattice, the number N of beads has to follow the relation $N = 3p^2 - 3p + 1$, where p is the number of beads on an edge. The experiments have been done with 547 beads, which corresponds to $p = 14$ beads per edge in the initial state. This configuration leads to a particle area density $\rho = 234\,000$ beads per m^2 and a filling fraction $\phi = 0.18$. The initial hexagonal lattice is built with a mask without agitation and under the desired magnetic field to stabilize the assembly of beads.

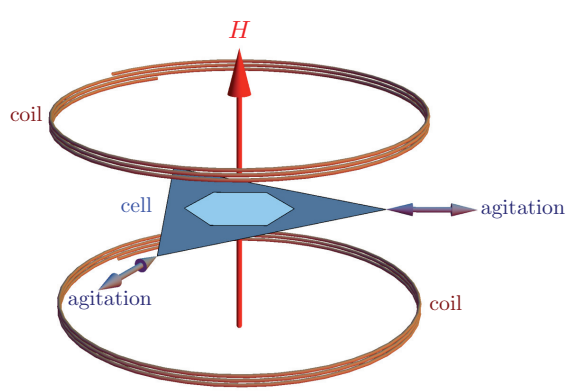

FIG. 1. (Color online) Sketch of the experimental setup composed of two coils used to produce a vertical homogeneous magnetic field H and a hexagonal cell, filled by 547 bead, agitated by two perpendicular loudspeakers. The cell is placed at the center of the coil.

After the initialization process, the agitation is switched on. After a relaxation time of 200 s, a CCD camera records a series of images at a fixed rate of 10 frames per second during 100 s. The resolution of the camera in the region of interest is 500 × 500 pixels. The system is backlighted with a lattice of LEDs and a diffuser. Therefore, the grains and the background appear, respectively, in black and white. A basic tracking method allows one to determine the position and the trajectory of each bead during the whole experiment. From the beads trajectories, one can determine the velocity of the beads, the mean square displacement, the pair correlation function, the orientational correlation function, and the dynamic Lindemann parameter. Determining the number of first neighbors and their mutual distance is essential to compute the orientational correlation function and the dynamic Lindemann criterion. Two methods are available to determine first neighbors of a particle: the Voronoi tesselation or the pair correlation function. Here, the pair correlation function has been used. Two particles are considered as first neighbors if the distance between them corresponds to the position of the first peak in the pair correlation function (see Sec. IV) including its width.

In this system, the magnetic interaction competes with the mechanical agitation. The magnetic interaction induces order while the agitation generates disorder. This competition is characterized by a dimensionless reduced temperature $T^\star$ (see definition in Sec. III). In all experiments, the strength of the agitation is fixed and the control parameter is the magnetic field strength.

III. REDUCED TEMPERATURE

The system used in this study is athermal, meaning that thermal agitation is not sufficient to move the beads. Therefore, an external source of agitation is needed. In order to produce a mechanical agitation comparable to a thermal agitation, some conditions must be verified concerning the diffusivity and the speed distribution. When the magnetic field is switched off, the beads are forming clusters. This behavior is commonly observed with shaken granular materials and is related to the dissipative character of the collisions [23]. Under weak interaction, the beads repel each other and the dissipative effects are attenuated. The characteristics of the agitation have been measured under these conditions.

To study the diffusivity of the beads in the system, the temporal evolution of the mean square displacement of the beads,

$$M(\tau) = \langle[\vec{r}(t+\tau) - \vec{r}(t)]^2\rangle, \tag{2}$$

has been used, where $\vec{r}(t)$ is the position of a specific bead at time t and $\langle\cdot\rangle$ represents an averaging over all the beads and many frames. This function behaves as $M(\tau) \sim \tau^\alpha$, where $\alpha = 2$ for ballistic motion, $2 > \alpha > 1$ for super diffusive motion, $\alpha = 1$ for diffusive motion, and $\alpha < 1$ for subdiffusive motion. Figure 2 shows the beads diffusivity for four typical values of the applied magnetic field (5250, 7000, 7700, 12 250 A/m) in a log-log plot. For a low magnetic field (5250 A/m), repulsion between two beads is strong enough to avoid direct collisions (dissipative collisions) and the beads are diffusive, like Brownian particles. Indeed, at short time, i.e., from 0.1 to

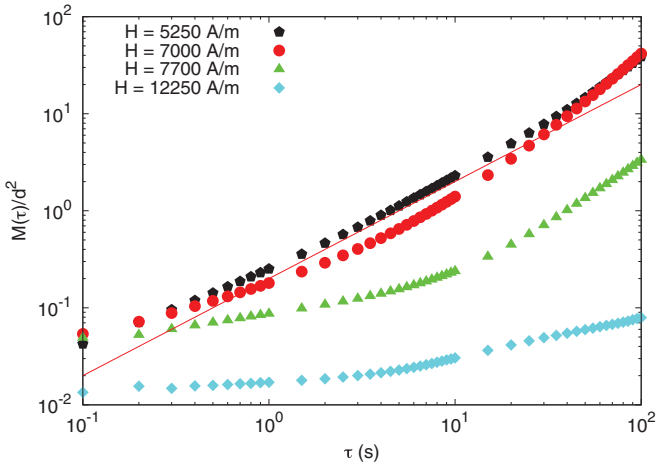

FIG. 2. (Color online) Mean square displacement for four values of the applied magnetic field: 5250, 7000, 7700, and 12 250 A/m (corresponding to $T^* = 0.2$, 0.1, 0.08, and 0.03). The solid line corresponds to a diffusive system.

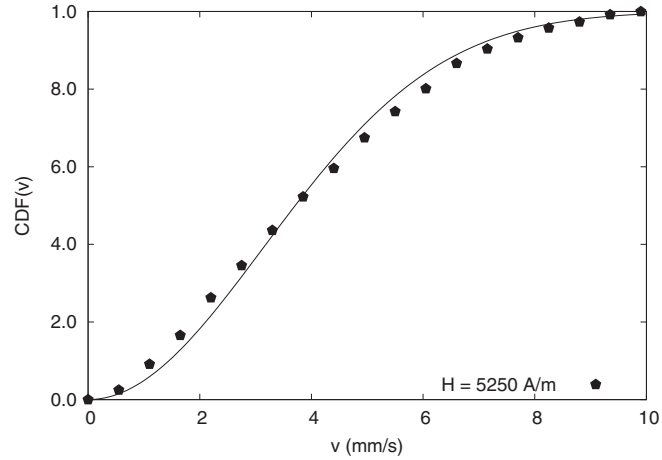

FIG. 3. Cumulate distribution of the bead speed for four values of the applied magnetic field: 5250, 7000, 7700, and 12 250 A/m (corresponding to $T^* = 0.2$, 0.1, 0.08, and 0.03). The plain curve is the Maxwell-Boltzmann cumulated distribution, given by Eq. (5).

10 s, the slope is close to 1, which is the signature of a diffusive behavior. The long time behavior is superdiffusive. Indeed, since the cell is not perfectly horizontal, the beads are sensitive to the gravity. Therefore, the beads are submitted to a diffusive motion related to both agitation and magnetic repulsion. In addition, a small drift of the particles, due to the gravity, is observed. For stronger magnetic field ($H > 5250$ A/m), a plateau emerges. Indeed, when the repulsion between two beads increases, the beads are caged by their neighbors. This caging effect affects the diffusivity of the beads and leads to a plateau in the mean square displacement [17].

In the 2D kinetic theory of gases, the particle speeds follow a Maxwell-Boltzmann distribution,

$$f(v) = \frac{v}{\alpha^2} \exp\left(-\frac{v^2}{2\alpha^2}\right), \tag{3}$$

with

$$\alpha = \sqrt{\frac{k_B T}{m}}. \tag{4}$$

The experimental cumulated speed distribution is presented in Fig. 3 for a low value of the applied magnetic field (5250 A/m). The theoretical curve is also plotted,

$$F(v) = 1 - \exp\left(-\frac{v^2}{2\alpha^2}\right). \tag{5}$$

The mean speed $\langle v \rangle$, which has been calculated from the tracking of the beads, is the only parameter of these curves. Indeed, by calculating the first moment of the distribution, the parameter α is related to the mean speed as

$$\langle v \rangle = \alpha \sqrt{\frac{\pi}{2}}. \tag{6}$$

Figure 3 shows the excellent agreement between theoretical curve using Eq. (5) and data.

The analysis of the beads' mean square displacement and speed distribution shows that the agitation is similar to a thermal agitation. The agitation energy $k_B T$ produced by the loudspeakers is estimated for $H = 5250$ A/m to avoid the formation of clusters. However, entropic effects prevail because this applied magnetic field produces weak interactions. From Eq. (4), Eq. (6), and the experimental measure of $\langle v \rangle$, the agitation energy per bead is estimated to be $m\alpha^2$ and is equal to 0.4×10^{-10} J. One can notice that the the measure of the mean kinetic energy per bead $\frac{1}{2} m \langle v^2 \rangle$ gives the same estimation.

The mean magnetic interaction energy between two beads is

$$\langle U \rangle = \frac{\mu_0}{4\pi} V^2 \chi_m^2 H^2 \left(\frac{\sqrt{3}}{2}\rho\right)^{3/2}, \tag{7}$$

where $(\frac{2}{\sqrt{3}}\frac{1}{\rho})^{1/2}$ corresponds to the typical distance between two beads in a 2D hexagonal lattice which has a particle area density ρ. This typical distance for the system is $2.22d$. The mean interaction energy has been estimated using magnetic properties of the beads from [22]. For an external magnetic field H from 7000 to 14 000 A/m, we find a mean interaction energy ranging from 0.51×10^{-10} to 3.6×10^{-10} J.

In order to quantify the competition between entropic effect and interaction effects in the system, a reduced temperature $T^\star$ is defined. This dimensionless parameter is the ratio between the agitation energy per bead and the mean interaction energy between two beads,

$$T^\star = \frac{k_B T}{\langle U \rangle}. \tag{8}$$

For an external magnetic field ranging from 7000 to 14 000 A/m, the reduced temperature $T^\star$ is situated between 0.1 and 0.02.

IV. EXPERIMENTAL RESULTS

The different states observed with the 2D assembly of magnetized grains are shown in Fig. 4 for typical values of the reduced temperature $T^\star$. The initial state of the system [Fig. 4(a)] can be considered as $T^\star = 0$ because the lack of agitation. This configuration presents a perfect translational symmetry and a sixfold symmetry which means a perfect

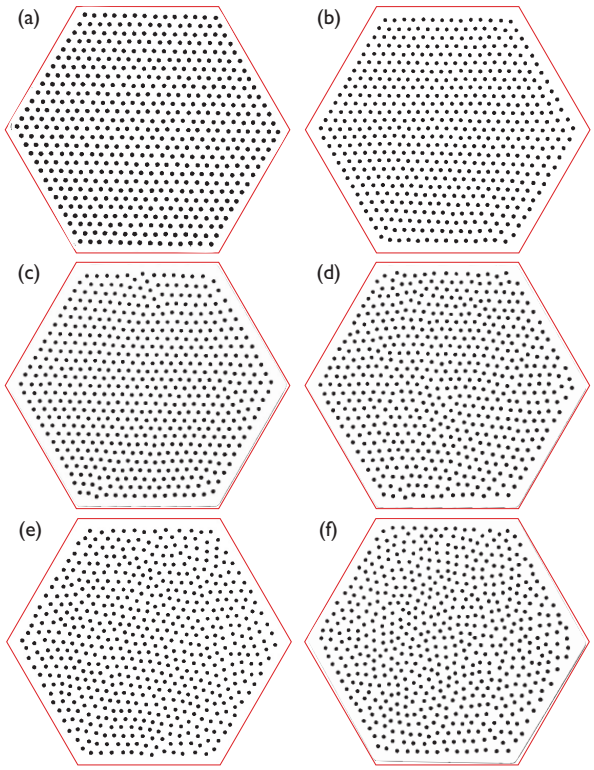

FIG. 4. (Color online) Snapshots of the system for the initial condition considered as $T^\star = 0$ (a) and for typical reduced temperature $T^\star = 0.02$ (b), $T^\star = 0.03$ (c), $T^\star = 0.06$ (d), $T^\star = 0.08$ (e), and $T^\star = 0.1$ (f).

translational and orientational order. A clear structural change is observed from $T^\star = 0.02$ to $T^\star = 0.1$. Indeed, for $T^\star = 0.02$ [Fig. 4(b)] and $T^\star = 0.03$ [Fig. 4(c)], the system exhibits a structure close to the perfect hexagonal lattice with a sixfold symmetry and with a translational symmetry at quasi-long range. For $T^\star = 0.06$ [Fig. 4(d)] and $T^\star = 0.08$ [Fig. 4(e)], the sixfold symmetry persists, but the translational symmetry vanishes. Finally, for $T^\star = 0.1$ [Fig. 4(f)] the system is completely disordered like a liquid state.

A fast Fourier transform of the real lattice obtained from snapshots in Fig. 4 enables us to study the pattern of Bragg scattering of the system in Fig. 5. For $T^\star = 0$ [Fig. 5(a)], the reciprocal lattice is hexagonal with a 30° rotation in comparison with the real lattice. At low reduced temperature $T^\star = 0.02$ [Fig. 5(b)] and $T^\star = 0.03$ [Fig. 5(c)], the pattern is close to a perfect hexagonal reciprocal lattice which indicates that the system has a sixfold symmetry. When $T^\star$ [Figs. 5(d) and 5(e)] increases, a sixfold symmetry is still observable but the spots become more blurred due to the loss of translation symmetry. For $T^\star = 0.1$ [Fig. 5(f)], spots become a ring, being the sign of the loss of sixfold symmetry as well.

These qualitative observations allow one to observe the phase transitions which will be quantified in the following. The translational order and the structure could be characterized by the pair correlation function

$$g(r) = \frac{1}{N}\left\langle \sum_{j\neq k} \delta(\vec{r} + \vec{r}_i - \vec{r}_k)\right\rangle. \tag{9}$$

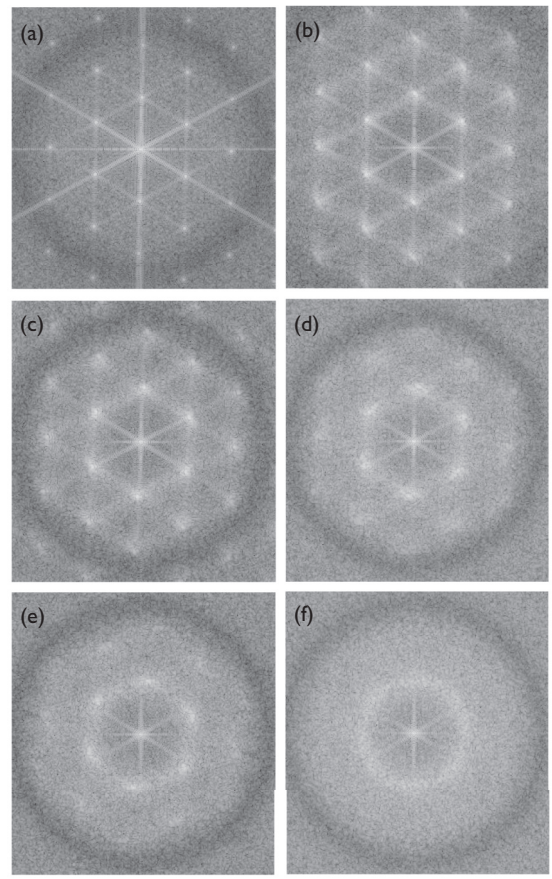

FIG. 5. Pattern of Bragg scattering of the system for the initial condition considered as $T^\star = 0$ (a) and for typical reduced temperature $T^\star = 0.02$ (b), $T^\star = 0.03$ (c), $T^\star = 0.06$ (d), $T^\star = 0.08$ (e), and $T^\star = 0.1$ (f).

This correlation function gives the probability to find two particles separated by a distance r. Even if $g(r)$ does not give a quantitative criterion for melting, this function is widely used to study translational order or structural changes upon a phase transition [9,16,24]. Figure 6 shows the pair correlation function $g(r)$ for typical reduced temperature. Vertical lines represent the six first peaks of $g(r)$ for a perfect hexagonal lattice. One can notice that the position of the first peak is $(\frac{2}{\sqrt{3}}\frac{1}{\rho})^{1/2} = 2.22$ as it is supposed to be in a 2D hexagonal lattice having a particle density area ρ. These peaks are sharp and their positions are following the sequence $r_1, r_2 = \sqrt{3}r_1, r_3 = 2r_1, r_4 = \sqrt{7}r_1, \ldots$. For low reduced temperature $T^\star = 0.02$ and $T^\star = 0.03$, the first peaks are well defined. Nevertheless, peaks widen for longer distance. This behavior is related to a quasi-long range translational order. When T^* increases, the peaks get broader and shorter because the probability tends to be uniform like a liquid. Thus, the second and the third peaks merge for $T^\star > 0.03$. Therefore, the translational order is vanishing, even at short range. Thus, the system is considered as melted. According to this criterion, the pair correlation function shows the loss of translational order, and so the melting, for a reduced temperature T^* included between 0.03 and 0.06. Let one notice that the pair correlation function does not give any information about the orientational order.

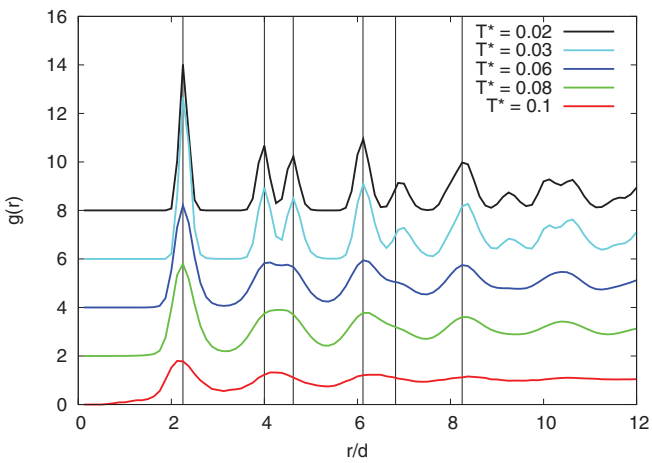

FIG. 6. (Color online) Pair correlation function $g(r)$ at $T^* = 0.02$, $T^* = 0.03$, $T^* = 0.06$, $T^* = 0.08$, and $T^* = 0.02$. The vertical lines correspond to the peaks of a perfect hexagonal lattice. Curves are shifted upwards when $T^\star$ decreases.

According to the KTHNY theory [3–7], the different states of a 2D system can be distinguished by translational and orientational order as summarized in Table I. These orders are respectively quantified with the translational correlation function

$$g_G(\vec{r} - \vec{r}') = \langle \exp\{i\vec{G} \cdot [\vec{u}(\vec{r}) - \vec{u}(\vec{r}')]\}\rangle \tag{10}$$

and the orientational correlation function

$$g_6(|\vec{r} - \vec{r}'|) = \langle \exp(6i[\theta(\vec{r}) - \theta(\vec{r}')]\rangle. \tag{11}$$

The vector $\vec{G}$ is a primary reciprocal lattice vector, $\vec{u}(\vec{r})$ is the displacement of a bead at the position $\vec{r}$ according to its ideal position in the lattice, and $\theta(\vec{r})$ represents the angle of the bond between two beads with respect to a determined direction. For 2D infinite crystals, the translational correlation function is expected to decrease algebraically $g_G(r) \sim r^{-\eta_G(T^\star)}$, with $\eta_G(T^\star) < 1/3$, and the orientational correlation function tends toward a finite value. For a hexatic phase, an exponentially decay is expected for $g_G(r)$ and an algebraic decay for $g_6(r) \sim r^{-\eta_6(T^\star)}$, where $\eta_6(T^\star) < 1/4$. For the liquid phase, both correlation functions decrease exponentially. The translational correlation function has not been computed because the reciprocal lattice is not precisely defined due to the lack of translational long range order [9]. Consequently, the reciprocal vector $\vec{G}$ cannot be determined precisely; nor can $g_G(r)$. The spatial orientational correlation function is represented in Fig. 7. One can see that for $T^* = 0.02$ and $T^* = 0.03$, $g_6(r)$ tends toward a constant and the system is considered as a crystal. For $T^* = 0.1$, $g_6(r)$ decays exponentially, indicating a short range orientational order, sign of a liquid state. For $T^* = 0.06$ and $T^* = 0.08$, one can see that $g_6(r)$ decays algebraically, a sign of quasi-long range orientational order. Then the system is in the hexatic phase. The limited number of beads restricts the quantitative comparison with the theoretical critical exponent η_6 and the clear distinction between the algebraic decay and the constant. However, the acquisition time is not limited. Thus, the temporal orientational correlation function $g_6(t)$ [11,25] enables a clear distinction

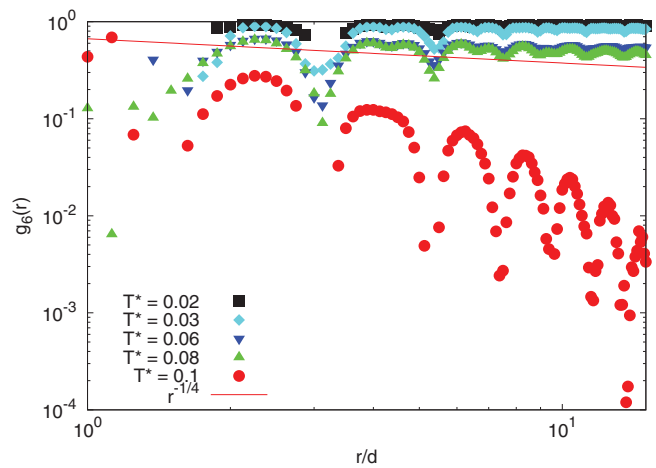

FIG. 7. (Color online) The orientational spatial correlation function $g_6(r)$ for typical reduced temperatures T^*. The blue curve represents an exponential decay which characterized a short range orientational order. The red curve represents an algebraical decay with an exponent equal to 1/4, which is the theoretical decay at the hexatic-liquid transition for an infinite system.

between solid and hexatic phase, even for a limited number of particles [26]. This correlation function is the temporal counterpart of the orientational correlation function $g_6(r)$. One has

$$g_6(t) = \langle \exp[i6\theta(t)]\rangle. \tag{12}$$

According to [25], in the hexatic phase, this function decreases algebraically with an exponent equal to $\eta_6(T^\star)/2$ In Fig. 8, the correlation function $g_6(t)$ is plotted for typical values of the reduced temperature $T^\star$. The behavior of the temporal correlation $g_6(t)$ is in agreement with the spatial counterpart $g_6(r)$. The curves corresponding to the critical exponents for an infinite system are plotted in Figs. 7 and 8.

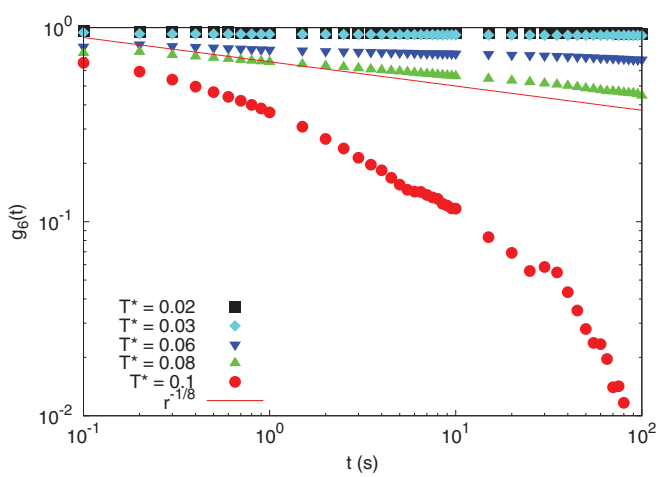

FIG. 8. (Color online) The orientational temporal correlation function $g_6(t)$ for typical reduced temperatures T^*. The red curve represents an algebraical decay with an exponent equal to $\frac{1}{8}$, which is the theoretical decay at the hexatic-liquid transition for an infinite system.

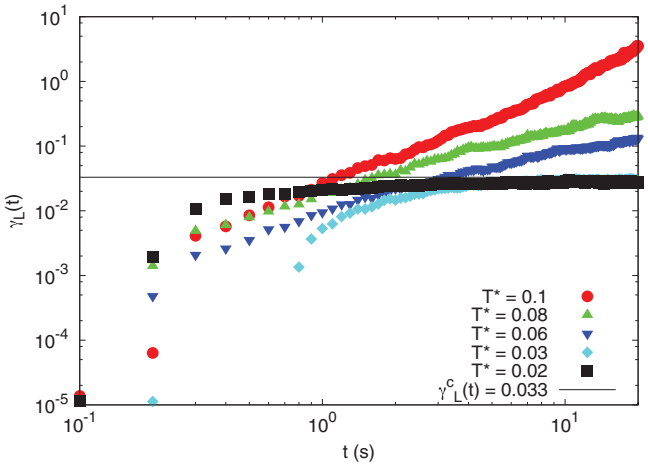

FIG. 9. (Color online) The dynamical Lindemann parameter for typical reduced temperature T^*. The black curve represents the critical value $\gamma_M^c = 0.033$ above which the system is considered as melted.

The Lindemann parameter is a typical criterion used to detect a melting transition [27]. This is defined as

$$\gamma_M = \langle(\vec{u}_j - \vec{u}_{j+1})^2\rangle/a^2, \tag{13}$$

where $\vec{u}$ is the particle displacement from its ideal position in the lattice as in Eq. (10). The indexes j and $j+1$ are corresponding to two neighboring particles and a corresponds to the typical distance between two beads in a 2D hexagonal lattice. In 2D, a system is melted for critical value $\gamma_M^c = 0.033$ [28]. Nevertheless, this criterion is obtained at equilibrium. This equilibrium state is reached after a long time. The Lindemann criterion has been generalized to a time-dependent criterion [10,11],

$$\gamma_L(t) = \langle(\Delta\vec{u}_j(t) - \Delta\vec{u}_{j+1}(t))^2\rangle/a^2, \tag{14}$$

where $\Delta\vec{u}(t) = \vec{u}(t) - \vec{u}(0)$. The limit of this function corresponds to γ_M. In a solid state, a particle does not keep away from its neighbors; thus, $\gamma_L(t)$ converges to a finite value. In a nonsolid state, the particles' motion is diffusive and $\gamma_L(t)$ diverges. At the melting point, $\gamma_L(t)$ converges to the critical value $\gamma_M^c = 0.033$ because at long time $\gamma_L(t)$ is close to γ_M. Figure 9 shows the behavior of such a function for typical reduced temperature T^*. For $T^* = 0.02$ and $T^* = 0.03$, the function tends to a finite value close to γ_M^c. Therefore, the system is in a solid state close to the melting point. For higher reduced temperatures, $\gamma_L(t)$ diverges. Then the system is melted but not necessarily in a liquid state.

V. DISCUSSION

The association of these correlation functions allows one to determine the state of the system and the phase transitions. For low values of the reduced temperature ($T^* = 0.02$ and $T^* = 0.03$), the behavior of $g(r)$ and $\gamma_L(t)$ give, respectively, a qualitative and quantitative criterion to detect a solid ordered state. In this range of $T^\star$, the system is solid and the reduced temperature corresponding to the transition is close to $T^* = 0.03$. Indeed, the dynamic Lindemann parameter $\gamma_L(t)$ tends to γ_M^c. In addition, both orientational correlation functions $g_6(r)$ and $g_6(t)$ tend to a constant indicating a long range orientational order. Therefore, according to the KTHNY theory (see Table I), the system is in a 2D crystal state.

For intermediate reduced temperature $0.06 \leqslant T^\star \leqslant 0.08$, the state of the system could be obtained through the orientational correlation functions $g_6(r)$ and $g_6(t)$. The algebraical decay is the signature of a quasi-long range orientational order. Moreover, the merging of the second and third peaks of $g(r)$ is a qualitative criterion that indicates the loss of translational order. According to the KTHNY theory, the transition from the hexatic to the liquid phase appears when $g_6(r)$ and $g_6(t)$ decay from algebraic to exponential. Therefore, the reduced temperature corresponding to this transition is between $T^\star = 0.08$ and $T^\star = 0.1$.

Finally, for higher reduced temperature ($T^* = 0.1$), the correlation functions $g_6(r)$ and $g_6(t)$ decay exponentially. The pair correlation function $g(r)$ shows a liquidlike structure. Moreover, the slope of $\gamma_L(t)$ is close to 1 as a perfect diffusive system. This corresponds to the liquid phase in the KTHNY theory.

Our results are in agreement with previous studies. Indeed, the melting in two stages has already been observed for athermal system with Coulomb interaction [18] even if a Coulomb interaction is a long range interaction in comparison with magnetic dipole-dipole interaction. Our experiments bear out that the results of the KTHNY theory are observable with an athermal system, even magnetic interaction. Moreover, the interest of developing a magnetic system is that magnetic interactions are better controlled than Coulomb interactions.

This confirmed that granular systems with appropriate agitation are also good model systems to study phase transition in 2D.

VI. CONCLUSION

In conclusion, we have developed a setup to study an athermal system where the magnetic dipole-dipole pair interaction and the agitation are controlled. Moreover, care has been taken to use agitation which leads to an erratic movement of the beads in agreement with the kinetic theory of gases. By adjusting the ratio between the kinetic energy of each bead and their pair interaction, the three phases (solid-hexatic-liquid) predicted by the KTHNY theory have been observed through both dynamic and static order parameter.

Despite its athermal and out of equilibrium character, the system described in this paper is in agreement with the KTHNY 2D melting theory. Thus, our experiment can be considered as a model system to study 2D crystals. Consequently, further investigations about bidimensional systems will be possible using this setup.

ACKNOWLEDGMENTS

G.L. would like to thank F.R.S.-FNRS for financial support. This work has been also supported by the INANOMAT Project (IAP P6/17) of the Belgian Science Policy. We thank O. Gerasimov and R. Messina for fruitful discussions.

[1] N. D. Mermin and H. Wagner, Phys. Rev. Lett. **17**, 1133 (1966).
[2] N. D. Mermin, Phys. Rev. **176**, 250 (1968).
[3] J. M. Kosterlitz and D. J. Thouless, J. Phys. C **6**, 1181 (1973).
[4] J. M. Kosterlitz, J. Phys. C **7**, 1046 (1974).
[5] B. I. Halperin and D. R. Nelson, Phys. Rev. Lett. **41**, 121 (1978).
[6] D. R. Nelson and B. I. Halperin, Phys. Rev. B **19**, 2457 (1979).
[7] A. P. Young, Phys. Rev. B **19**, 1855 (1979).
[8] A. H. Marcus and S. A. Rice, Phys. Rev. Lett. **77**, 2577 (1996).
[9] A. Brodin, A. Nych, U. Ognysta, B. Lev, V. Nazarenko, M. Skarabot, and I. Musevic, Condens. Matter Phys. **13**, 33601 (2010).
[10] K. Zahn, R. Lenke, and G. Maret, Phys. Rev. Lett. **82**, 2721 (1999).
[11] K. Zahn and G. Maret, Phys. Rev. Lett. **85**, 3656 (2000).
[12] P. Bladon and D. Frenkel, Phys. Rev. Lett. **74**, 2519 (1995).
[13] L. Assoud, F. Ebert, P. Keim, R. Messina, G. Maret, and H. Lowen, J. Phys.: Condens. Matter **21**, 464114 (2009).
[14] J. S. Olafsen and J. S. Urbach, Phys. Rev. Lett. **95**, 098002 (2005).
[15] F. Moucka and I. Nezbeda, Phys. Rev. Lett. **94**, 040601 (2005).
[16] P. M. Reis, R. A. Ingale, and M. D. Shattuck, Phys. Rev. Lett. **96**, 258001 (2006).
[17] P. M. Reis, R. A. Ingale, and M. D. Shattuck, Phys. Rev. Lett. **98**, 188301 (2007).
[18] X. H. Zheng and R. Grieve, Phys. Rev. B **73**, 064205 (2006).
[19] M. Saint Jean, C. Guthmann, and G. Coupier, Eur. Phys. J. B **39**, 61 (2004).
[20] F. Boyer and E. Falcon, Phys. Rev. Lett. **103**, 144501 (2009).
[21] K. J. Strandburg, Rev. Mod. Phys. **60**, 161 (1988).
[22] B. M. Shah, J. J. Nudell, K. R. Kao, L. M. Keer, Q. J. Wang, and K. Zhou, J. Sound Vib. **330**, 182 (2011).
[23] E. Opsomer, F. Ludewig, and N. Vandewalle, Europhys. Lett. **99**, 40001 (2012).
[24] R. Messina and H. Lowen, Phys. Rev. E **73**, 011405 (2006).
[25] D. R. Nelson, in *Phase Transition and Critical Phenomena*, edited by C. Domb and J. L. Lebowitz (Academic Press, London, 1983).
[26] G. Coupier, C. Guthmann, Y. Noat, and M. Saint Jean, Phys. Rev. E **71**, 046105 (2005).
[27] F. A. Lindemann, Phys. Z. **11**, 609 (1910).
[28] V. M. Bedanov and G. V. Gadiyak, Phys. Lett. A **109**, 289 (1985).